

A Finite Element Approach for Trajectory Optimization in Wire-Arc Additive Manufacturing

Johannes Schmidt
Johannes Buhl
Armin Fügenschuh

A Finite Element Approach for Trajectory Optimization in Wire-Arc Additive Manufacturing

Johannes Schmidt ^{a*} Johannes Buhl ^a Armin Fügenschuh ^a

July 26, 2021

Abstract

In wire-arc additive manufacturing (WAAM), the desired workpiece is built layer-wise by a moving heat source depositing droplets of molten wire on a substrate plate. To reduce material accumulations, the trajectory of the weld source should be continuous, but transit moves without welding, called deadheading, are possible. The enormous heat of the weld source causes large temperature gradients, leading to a strain distribution in the welded material which can lead even to cracks. In summary, it can be concluded that the temperature gradient reduce the quality of the workpiece. We consider the problem of finding a trajectory of the weld source with minimal temperature deviation from a given target temperature for one layer of a workpiece with welding segments broader than the width of the weld pool. The temperature distribution is modeled using the finite element method. We formulate this problem as a mixed-integer linear programming model and demonstrate its solvability by a standard mixed-integer solver.

Keywords: additive manufacturing, mixed-integer linear programming, finite element method, heat equation, path optimization

1 Introduction

In the last decades, the field of additive manufacturing (AM) developed into an advantageous alternative to common metal cutting manufacturing processes, due to its ability to produce complex workpieces without substantial material removal. One of these processes is the so-called wire-arc additive manufacturing (WAAM). In this process, a wire is molten by an electrical arc or laser and deposited in droplets on an underlying substrate plate building the workpiece layer-wise. The weld source moves around freely and is capable of transiting without welding, called deadheading. A crucial factor to the quality of the manufactured workpiece is the trajectory of the weld source. Due to its enormous heat, high thermal gradients can occur, leading to stress inside the material. Possible results are distortions of the workpiece or even cracks. Controlling the temperature gradients and aiming for a homogeneous temperature distribution within the workpiece reduces these effects. Therefore, detailed planning of the welding trajectory is advantageous. A review about the effect of the chosen weld strategy to the process time and workpiece quality can be found in [3]. We tackle the problem of finding a path of the weld source with minimal absolute deviation to a given target temperature for a single layer of the workpiece. In [4], the strain simulation for a given welding trajectory using a finite element

^aBrandenburg University of Technology Cottbus-Senftenberg,
Platz der Deutschen Einheit 1, 03046 Cottbus, Germany,
{johannes.schmidt,johannes.buhl,fuegenschuh}@b-tu.de

*Corresponding author

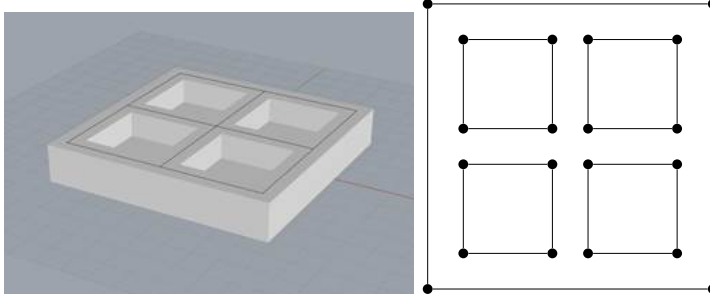


Figure 1: A prototypical workpiece (*left*) and a single layer of it (*right*)

method is presented. For workpieces with wall strength as broad as the width of the weld pool, the problem has been studied in [1]. Thus, we consider in this work wall strengths broader than the width of the weld pool, motivated in [5]. A mixed-integer linear problem is set up to compute the trajectory and track the temperature during the process at the same time. The temperature distribution within the workpiece is affected by the heat input of the weld source, heat conduction, and thermal radiation. These three aspects are combined in the heat equation with a Robin boundary condition. It is discretized using the finite element method and incorporated into the model. Its solvability by a standard mixed-integer solver is demonstrated on a test instance.

2 Mathematical Model

Given the structure of the desired workpiece, the two-dimensional layers are obtained by slicing it vertically, see Fig. 1. Each layer consists of segments that have to be welded and intersection points between them. Thus, every layer can be considered as an undirected graph $G = (\mathcal{V}, \mathcal{W})$, with nodes at the intersection points and the segments between them as edges. This graph has not to be connected and can contain several components $G_i = (\mathcal{V}_i, \mathcal{W}_i)$ ($i = 1, \dots, n$). Let \mathcal{V}^{odd} and \mathcal{V}_i^{odd} denote the set of nodes with odd degree in G or its component G_i , respectively.

In practical application, the heat source is much slower while welding than during deadheading. Thus, we assume that transition moves are done immediately without consuming time. Since the movement speed v_w of the heat source while welding and the length $l_{i,j}$ of each segment $(i, j) \in \mathcal{W}$ is known a priori, the time to weld the complete layer is given by $T = \sum_{(i,j) \in \mathcal{W}} \frac{l_{i,j}}{v_w}$. Introducing the time step length Δt , the time horizon $[0, T]$ is discretized as a set of discrete time steps $\mathcal{T}_0 = \{0, 1, \dots, T^{max}\}$, with $T^{max} = \sum_{(i,j) \in \mathcal{W}} \tau_{i,j} = \sum_{(i,j) \in \mathcal{W}} \left\lceil \frac{l_{i,j}}{v_w \Delta t} \right\rceil$ and $\tau_{i,j}$ describing the time to weld segment $(i, j) \in \mathcal{W}$. As abbreviations we use $\mathcal{T} = \mathcal{T}_0 \setminus \{0\}$, $\mathcal{T}^- = \mathcal{T} \setminus \{T^{max}\}$, and $\mathcal{T}_0^- = \mathcal{T}_0 \setminus \{T^{max}\}$.

2.1 Path Generation

Modeling each layer as an undirected graph, the search for a welding trajectory of the heat source becomes the problem of computing a continuous path for the graph, a problem closely related to the Chinese Postman problem [2], where the artificial edges are now the deadheading moves. The number of the necessary artificial edges ω in the solution of the Chinese Postman problem for a connected graph G is $\omega = \frac{|\mathcal{V}^{odd}|}{2}$. In our setting, the start and the endpoint of the path can be different. Thus, the number of necessary deadheading moves within each component can be calculated by $\omega_i = \frac{|\mathcal{V}_i^{odd}|}{2} - 1$. Furthermore, there are $n - 1$ moves necessary to navigate between the components. In total, the number of necessary deadheading moves for the whole graph G is given by $\sum_{i=1}^n \omega_i + n - 1$.

Let $\mathcal{U} \subseteq \mathcal{V} \times \mathcal{V}$ denote the set of all possible deadheading moves. All segments can be welded in arbitrary direction, thus the set \mathcal{W} is extended to $\overline{\mathcal{W}} = \{(i, j) \in \mathcal{W} \mid (i, j) \in \mathcal{W} \vee (j, i) \in \mathcal{W}\}$ and we introduce further sets $\mathcal{W}^* = \{(i, t_i, j, t_j) \in \mathcal{V} \times \mathcal{T}_0 \times \mathcal{V} \times \mathcal{T} \mid (i, j) \in \overline{\mathcal{W}}, t_j = t_i + \tau_{i,j}\}$ and $\mathcal{U}^* = \{(i, j, t) \in \mathcal{U} \times \mathcal{T}^-\}$ to relate all welding and deadheading moves to the time, respectively. Let $w_{i,t_i,j,t_j} \in \mathcal{W}^*$ be a binary variable indicating if segment $(i, j) \in \overline{\mathcal{W}}$ is processed from time step $t_i \in \mathcal{T}_0$ to time step $t_j \in \mathcal{T}$ and $u_{i,j,t} \in \mathcal{U}^*$ a binary variable indicating if connection $(i, j) \in \mathcal{U}$ is used for deadheading at time step $t \in \mathcal{T}^-$. Then, the problem of finding a welding path can be stated as

$$\sum_{i,j,t_j:(i,0,j,t_j) \in \mathcal{W}^*} w_{i,0,j,t_j} = 1, \quad (1)$$

$$\sum_{i,t_i,j:(i,t_i,j,T^{max}) \in \mathcal{W}^*} w_{i,t_i,j,T^{max}} = 1, \quad (2)$$

$$\sum_{t_i,t_j:(i,t_i,j,t_j) \in \mathcal{W}^*} w_{i,t_i,j,t_j} + \sum_{t_j,t_i:(j,t_j,i,t_i) \in \mathcal{W}^*} w_{j,t_j,i,t_i} = 1 \quad \forall (i, j) \in \mathcal{W}, \quad (3)$$

$$\begin{aligned} & \sum_{h,t_h:(h,t_h,i,t) \in \mathcal{W}^*} w_{h,t_h,i,t} + \sum_{h:(h,i,t) \in \mathcal{U}^*} u_{h,i,t} \\ &= \sum_{j,t_j:(i,t,j,t_j) \in \mathcal{W}^*} w_{i,t,j,t_j} + \sum_{j:(i,j,t) \in \mathcal{U}^*} u_{i,j,t} \quad \forall i \in \mathcal{V}, t \in \mathcal{T}, \quad (4) \end{aligned}$$

$$\sum_{(i,j,t) \in \mathcal{U}^*} u_{i,j,t} = \omega + n - 1, \quad (5)$$

$$\sum_{i,j:(i,j,t) \in \mathcal{U}^*} u_{i,j,t} \leq 1 \quad \forall t \in \mathcal{T}. \quad (6)$$

The weld source has to start and end its path somewhere (1), (2), while every segment must be welded (3). The computed path has to be continuous (4) and the number of deadheading moves is limited (5). Equation (6) is not necessary, but a valid inequality since every time there are two consecutive deadheading moves $(i, j, t), (j, k, t) \in \mathcal{U}^*$ in one time step, they can be merged to $(i, k, t) \in \mathcal{U}^*$ reducing the traveled distance.

2.2 Temperature Distribution

To model the temperature distribution within one layer of the workpiece during the welding process, the heat input of the weld source, heat conduction, and thermal radiation have to be taken into account. The two dimensional heat equation

$$\frac{\partial \theta}{\partial t}(x, y, t) = \alpha \left(\frac{\partial^2 \theta}{(\partial x)^2}(x, y, t) + \frac{\partial^2 \theta}{(\partial y)^2}(x, y, t) \right) + q(x, y, t) \quad \forall (x, y) \in \Omega, t \in (0, T], \quad (7.1)$$

$$\frac{\partial \theta}{\partial n}(x, y, t) = \kappa^e \left(\theta^{amb}(t) - \theta(x, y, t) \right) \quad \forall (x, y) \in \partial\Omega, \forall t \in [0, T], \quad (7.2)$$

$$\theta(x, y, 0) = \theta^{init}(x, y) \quad \forall (x, y) \in \Omega, \quad (7.3)$$

describes the heat conduction within an area Ω with initial temperature distribution θ^{init} and ambient temperature θ^{amb} . The Robin boundary condition (7.2) allows a linear approximation of the thermal radiation [1].

To discretize the heat equation (7), $\tau_{i,j} - 1$ nodes are added equidistantly on every segment $(i, j) \in \mathcal{W}$ and collected in the set \mathcal{V}^{int} . To relate these interior nodes to their corresponding segment, a function $\xi : \mathcal{V}^{int} \mapsto \mathcal{W} \times \{1, \dots, \tau_{i,j} - 1\}$ is introduced, reporting the respective segment and the nodes position along it for every interior node. Furthermore, let the variable $\theta_{i,t}$ describe the temperature of node $i \in \overline{\mathcal{V}} := \mathcal{V} \cup \mathcal{V}^{int}$ at time step

$t \in \mathcal{T}_0$. We apply the finite element method according to [6] with node set $\bar{\mathcal{V}}$, the segments $(i, j) \in \mathcal{W}$ as boundary of the area Ω , and linear triangle elements. This yields the linear equation system

$$(M + \Delta t K) \vec{\theta}_{t+1} = \Delta t (\vec{q}_{t+1} f^{\vec{H}} + f^{\vec{R}}) + M \vec{\theta}_t, \quad (8)$$

with mass matrix $M = (m_{i,j})_{i,j}$, stiffness matrix $K = (k_{i,j})_{i,j}$, load vectors $f^{\vec{H}}$ and $f^{\vec{R}}$, and $\vec{\theta}_t, \vec{q}_t$ describing the vectors of the temperature and the heat input of all nodes at time step $t \in \mathcal{T}_0^-$, respectively.

The weld source is described by the piece-wise constant approximation of the Goldak heat source model from [1] with coefficients κ_k^w , $k = 1, \dots, K^w$ and intervals \mathcal{P}_k . The temperature gain of a node at the center of the weld pool is given by the parameter φ^w . To simplify notations, the binary variable $w_{i,t}$ with

$$w_{i,t} = \begin{cases} \sum_{h,t_h:(h,t_h,i,t) \in \mathcal{W}^*} w_{h,t_h,i,t} + \sum_{h:(h,i,t) \in \mathcal{U}^*} u_{h,i,t} & , i \in \mathcal{V}, t \in \mathcal{T}_0, \\ \sum_{\substack{(h,t_h,j,t_j) \in \mathcal{W}^* \\ \xi(i)=(h,j,k) \\ t=t_h+k}} w_{h,t_h,j,t_j} + \sum_{\substack{(j,t_j,h,t_h) \in \mathcal{W}^* \\ \xi(i)=(h,j,k) \\ t=t_h-k}} w_{j,t_j,h,t_h} & , i \in \mathcal{V}^{int}, t \in \mathcal{T}, \\ 0 & , i \in \mathcal{V}^{int}, t = 0, \end{cases} \quad (9)$$

is introduced, indicating above which node $i \in \bar{\mathcal{V}}$ the weld source is positioned at time step $t \in \mathcal{T}_0$. Note that the third case is necessary since the index sets of the sums in (9) are empty for $i \in \mathcal{V}^{int}$ at $t = 0$. The temperature gain of the nodes from the weld source is then given by

$$\varphi_{i,t} = \sum_{k=1}^{K^w} \sum_{\substack{j \in \mathcal{V} \cup \mathcal{V}^{int} \\ d_{i,j}^e \in \mathcal{P}_k}} \kappa_k^w \varphi^w w_{i,t} \quad \forall i \in \bar{\mathcal{V}}, \forall t \in \mathcal{T}_0, \quad (10)$$

where $d_{i,j}^e$ is the Euclidean distance between nodes $i, j \in \bar{\mathcal{V}}$. Let θ_i^{init} denote the initial temperature of node $i \in \bar{\mathcal{V}}$. Incorporating (10) into (8), the temperature distribution within the workpiece is modeled by

$$\theta_{i,0} = \theta_i^{init}, \quad \forall i \in \bar{\mathcal{V}} \quad (11)$$

$$\sum_{j \in \bar{\mathcal{V}}} (m_{i,j} + \Delta t k_{i,j}) \theta_{j,t} = \sum_{j \in \bar{\mathcal{V}}} m_{i,j} \theta_{j,t-1} + \Delta t (\varphi_{i,t} f_i^H + f_i^R) \quad \forall i \in \bar{\mathcal{V}}, t \in \mathcal{T}. \quad (12)$$

The initial temperature of each node is set in (11) and then the linear equation system (12) is solved for every time step.

To achieve a preferably homogeneous temperature distribution, we minimize the absolute deviation of the temperature of the workpiece to a given target temperature θ^{tar} . Introducing further variables $\theta_{i,t}^+, \theta_{i,t}^- \in \mathbb{R}_+$ to describe the positive and negative portion of the absolute value function, the objective function is given by

$$\min \sum_{i \in \bar{\mathcal{V}}, t \in \mathcal{T}_0} \theta_{i,t}^+ + \theta_{i,t}^- \quad (13)$$

with the additional constraint

$$\theta^{tar} - \theta_{i,t} = \theta_{i,t}^+ - \theta_{i,t}^- \quad \forall i \in \bar{\mathcal{V}}, t \in \mathcal{T}_0. \quad (14)$$

3 Computational Results and Conclusions

The mixed-integer model consisting of constraints (1) – (6), (11), (12), (14), and objective (13) is implemented in AMPL using CPLEX 12.10 (default settings) for its solution

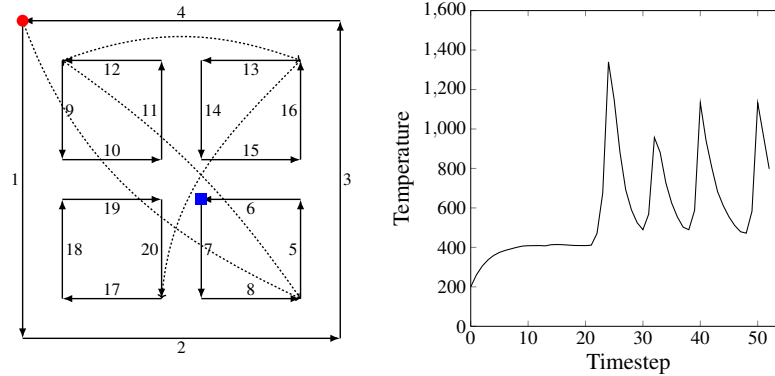


Figure 2: Optimal welding path for the considered layer (*left*) and temperature progression of node 12 (*right*). The weld trajectory is given by the numbers next to each segment. Dashed lines describe deadheading moves, the starting point of the path is marked by a red circle, and node 12 by a blue square

on a Mac Pro with an Intel Xeon W running 32 threads parallel at 3.2 GHz clockspeed and 768 GB RAM. As an example instance, the layer displayed in Fig. 1 is used with a side length of 16 mm and inner squares of 5×5 mm. The parameter values are chosen according to [1], except for $\kappa^e = 0.5$ and $\theta^{tar} = \theta^{amb}(t) = 200^\circ\text{C}$, which are estimated. After 172,670 seconds, the optimal solution was obtained. It is displayed in Fig. 2, together with the temperature progression of node 12, where all aspects of heat transmission are observable. In the beginning, its temperature increases due to heat conduction through the material. The weld source reaches this node at time step 24, leading to a first peak in its temperature progression. With this high temperature, the effect of heat conduction is outperformed by the heat loss due to radiation. Later, there is a significant temperature gain every time the node is within the area of effect of the weld source.

In our future work, we formulate new objective functions providing better solutions of the LP relaxation during the solution process. Furthermore, we consider workpieces where the wall strength of every segment can be arbitrary and extend the problem to several consecutive layers, where the chosen paths for each layer should differ to increase the stability of the workpiece and avoid joints.

References

- [1] Martin Bähr, Johannes Buhl, Georg Radow, Johannes Schmidt, Markus Bambach, Michael Breuß, and Armin Fügenschuh. Stable honeycomb structures and temperature based trajectory optimization for wire-arc additive manufacturing. *Optimization and Engineering*, 22(2):913–974, 2021.
- [2] J. Edmonds and E. L. Johnson. Matching, Euler tours and the chinese postman. *Mathematical Programming*, 5:88–124, 1973.
- [3] Jingchao Jiang and Yongsheng Ma. Path planning strategies to optimize accuracy, quality, build time and material use in additive manufacturing: a review. *Micromachines*, 11(7):633, 2020.
- [4] Filippo Montevecchi, Giuseppe Venturini, Niccolò Grossi, Antonio Scippa, and Gianni Campatelli. Finite element mesh coarsening for effective distortion prediction in wire arc additive manufacturing. *Additive Manufacturing*, 18:145–155, 2017.

- [5] Lam Nguyen, Johannes Buhl, and Markus Bambach. Continuous eulerian tool path strategies for wire-arc additive manufacturing of rib-web structures with machine-learning-based adaptive void filling. *Additive Manufacturing*, 35:101265, 2020.
- [6] Jan Taler and Pawel Ocloń. Finite element method in steady-state and transient heat conduction. *Encyclopedia of thermal stresses*, 4:1604–1633, 2014.

IMPRESSUM

Brandenburgische Technische Universität Cottbus-Senftenberg
Fakultät 1 | MINT - Mathematik, Informatik, Physik, Elektro- und Informationstechnik
Institut für Mathematik
Platz der Deutschen Einheit 1
D-03046 Cottbus

Professur für Ingenieurmathematik und Numerik der Optimierung
Professor Dr. rer. nat. Armin Fügenschuh

E fuegenschuh@b-tu.de
T +49 (0)355 69 3127
F +49 (0)355 69 2307

Cottbus Mathematical Preprints (COMP), ISSN (Print) 2627-4019
Cottbus Mathematical Preprints (COMP), ISSN (Online) 2627-6100

www.b-tu.de/cottbus-mathematical-preprints
cottbus-mathematical-preprints@b-tu.de
doi.org/10.26127/btuopen-5575